TECHNICAL PAPER

Study of Tribological Properties of Nano-Sized Red Mud Particle-Reinforced Polyester Composites

S. Richard[1] · J. SelwinRajadurai[2] · V. Manikandan[3] · M. Chithambara Thanu[1] ·
V. Arumugaprabu[3] · R. Deepak Joel Johnson[3]

Abstract Red mud (RM) in powder form is a waste substance obtained during extraction of pure alumina from Bauxite ore by Bayer's method. In this work, this red mud is used as reinforcement in nano-sized particulate form in the unsaturated polyester matrix. The mean particle size of 720 nm, 612 nm, 475 nm, 263 nm, and 110 nm were produced by ball milling for the milling period of 6–30 h. The composites were prepared by varying the size of the particle and for different particle weight fraction of 0.5, 1.0, 1.5, 2.0 and 2.5 wt.%. The wear characteristics of these red mud particulate composites were studied, and the effect of the particle size variation and particle weight fraction were reported. Particle size and particle content were observed to play a major part in frictional characteristics of the composites. The reduction in specific wear rate was 47.72% for 110 nm particle size composite sample with a weight fraction of 2.5 wt.%, and it showed 39.28% reduction in coefficient of friction on comparing with that of pure cured polyester resin. Red mud particles were characterized by FTIR, XRD and AFM analysis. Worn-out surfaces were analyzed by scanning electron microscope (SEM) for morphological study.

1 Introduction

Recently, nanocomposites gained greater attraction. A large number of scientist and environmentalist has exhibited stupendous interest in composites since they possess extremely good and distinctive characters. [1–4]. Efforts are being underway by the scientist to control the nanostructures through the use of innovative synthetic and systematic approaches. They have a high surface to volume ratio and aspect ratio, and hence, they are ideal to be used as potential filler or reinforcement in polymers. Polymer properties can be improved moderately to considerable value by incorporating particulate fillers or fibers or filler/fiber combination as reinforcements which give birth to polymer composites. Due to good strength to weight ratio, the polymer composites become a good substitute for metals and they are largely employed in automobile, aerospace and many corrosion prevention engineering application/components [5, 6]. Polymer composites emerged as a classic material since it can be tailored to the suitable requirement, ease of manufacturing even for a single component and mainly because of its high specific strength as well as the high specific modulus. When the reinforcement material is of particle nature, the derived composites are termed as a particulate composite. In this type of particulate composite, the reinforcement's particles are approximately in spherical form.

Nanocomposite properties rely not only on the properties of the particular parent material but also on their morphology and interfacial characteristics. Size and shape of the particle, volume or weight fraction, their level of

✉ V. Manikandan
  vaimanikandan@yahoo.com

1 Mechanical Engineering Department, Sivanthi Aditanar College of Engineering, Tiruchendur, Tamil Nadu 628215, India

2 Mechanical Engineering Department, Government College of Engineering, Tirunelveli, Tamil Nadu 627007, India

3 Department of Mechanical Engineering, Kalasalingam Academy of Research and Education, Krishnankoil, Tamil Nadu 626126, India

dispersion, dispersion pattern, the particle matrix interaction and the presence of voids are the main parameters which determine the properties of particulate polymer composites [7]. The influence of red mud on banana polyester composites was reported [8, 9]. Akinci et al. [10] reported that the increase in red mud volume increases the crystallization effect of the polymer through X-ray diffraction study.

The magnitude of industrial wastes accumulated over the surface of the earth is increasing day by day in large quantities during the recent years. Reducing the quantity of hazardous industrial waste and thereby reducing environmental pollution is of great concern for environmentalists and researchers today which is feasible by converting the waste into useful materials suitable for different applications. Several researchers have strived hard in using different industrial wastes in fabricating composite materials which minimize the environmental pollution caused by the hazardous waste materials which are also inexpensive [11, 12]. This will lead to a reduction in the presence of hazardous material on the surface of the earth and thereby making this globe a safer place to live.

Use of nano-sized particles in the form of reinforcement, filler and also fiber/filler combination in polymer matrix to improve specific properties such as void reduction, to change viscosity and melting temperature, thermal stability, toughness and hardness adhesion resistance are currently focused by many materials researchers, technologists, design engineer and industrial engineer [13–15]. Nanoparticle when used as filler in polymer composites, it imparts with good wear resistance properties to the polymer materials [16–18]. High surface area contact of the nano-sized particle is the main attractive reason for being used in composites. Due to the high surface area of the particles, the inter-phase in the composite is extremely large and this leads to the strong bonding of the matrix with the fillers which results in the enhancement of frictional properties even with an extremely low filler loading [17]. The nanoparticle as reinforcement in polymer composites is a new category of material in which their properties are improved considerably even at very low volume fraction [19–22]. There was a considerable improvement in tribological properties of the polymer due to the addition of nanoparticle such as TiO_2, Al_2O_3, biochar, CuO, ZnO, ZrO_2, SiC, Fe_2O_3, etc., as reported by researchers [23–28].

Red mud is an insoluble waste in aluminum industries obtained from bauxite ore during the extraction of alumina (Al_2O_3) by Bayer's process worldwide. Around 1.5 to 2.5 tonnes of red mud is produced for every tonne of alumina formed whose quantity depends upon the source of bauxite ore [29]. In India, around 2 million tonnes of red mud is being produced annually, whereas globally it is around 70 million tonnes per annum and currently the global inventory of red mud is around 2.7 billion tonnes [23, 30]. This enormous quantity of red mud produced is discarded into holding ponds and dumping yards by the industries and is an environmental hazard which turns the fertile lands infertile and causes respiratory diseases to the people. In spite of several disposal methods available, the scientist and engineers around the globe are striving hard to obtain a viable solution either to dispose or to reuse the red mud. This slurry when dried becomes powdered form. The Red mud which is in the powdered form obtained from the bauxite by different methods is applicable to be used in construction applications because of its good properties [31–33].

In the present study, red mud, an industrial waste has been used as reinforcement in an unsaturated polyester resin matrix. It has mainly been focused on the tribological behavior when the particle is at nano-size and its effect is prominent especially at low levels of red mud content. Various nano-sized red mud particulate at a different weight percentage ranging from 0% to 2.5% was considered. The tribological properties were studied by carrying out sliding wear tests. The morphological studies were carried out by optical microscopy and scanning electron microscope (SEM) on the wear tested composite samples. The present study revealed the tribological properties of the nano-sized red mud particle which was reinforced to polyester composites.

2 Experimental Methodology

2.1 Materials

Polyester resin (unsaturated) with molecular formula ($C_8H_6O_2$, $C_8H_{16}O_4$, $C_5H_{12}O_2$, $C_4H_2O_3$)n has been used as matrix material for fabrication of polymer composite in this research work. In the present research work, the collected red mud was milled into various sizes at nano-level and used as the reinforcement.

2.1.1 Polyester Resin (Unsaturated)

The polyester resin (unsaturated) which is commercially available in the trade name Shree polymer has been used as the matrix for this work. Methyl ethyl ketone peroxide (MEKP) and cobalt naphthenate were used as the catalyst and the accelerator, respectively. They were obtained from Shrinithi Chemicals, Tirunelveli, Tamil Nadu.

2.1.2 Red Mud

The mean particle size of Red mud is about 80–100 μm and is brick red in color. It constitutes iron, silica, titanium

as a part of the parent ore and a few other minor elements. It is thixotropic, alkaline and possesses a huge surface area ranging between 13 and 16 m^2/g with a density of 2.53 g/cm^3. It also has a wide range of components such as Al_2O_3, Fe_2O_3, Na_2O, SiO_2, FeS, CaO, TiO_2 which depends on the source. The red mud used in this research work as shown in (Fig. 1) was collected from the MALCO alumina plant yards at Mettur in Tamil Nadu, India.

Red mud collected from the yard was cleaned to remove the foreign material and ground to fine size in a planetary ball mill with ball mill ratio of 1:10, i.e., 1000 g of balls were used to mill 100 g of red mud. In this study, the red mud was milled for a time duration varying from 6 to 30 h. Fine particles of red mud ball milled for 18 h is shown in Fig. 1 which was captured using Sony cyber shot camera. Varying upon the milling duration, particles with varied sizes were obtained. The mean particle size of the milled red mud particle was measured using Horiba SZ-100 by particle analyzer with standard distribution. The particle size of the red mud has been represented by scattered light intensity. Holder temperature was maintained at 25 °C. Scattering angle for Red mud particle was measured as 173°. It is said from the principle of particle size analysis by laser diffraction that higher the angle of light scattering, the smaller the particle size. The particle size obtained by this process was measured as 720 nm for 6-h milling, 612 nm for 12-h milling, 475 nm for 18-h milling, 263 nm for 24-h milling and 110 nm for 30-h-milled powder. Figure 2 shows the distribution of particle size of red mud particles milled for 18 h measured by particle analyzer in the form of the distribution curve.

A considerable decrease in mean particle size, with an increase in the duration of milling hours was evident and is portrayed in the graph shown in Fig. 3. SEM–EDAX of the Red mud particle is shown in Fig. 4. It was found that oxygen and carbon were the major contributor with 47.3 wt.% and 24.5 wt.%. Red mud particle also contains 12.3 wt.% of Iron (Fe), 6.3 wt.% of Aluminum (Al), 5.3 wt.% of Sodium (Na), 2.7 wt.% of Si, 0.9 wt.% of Ca and 0.6 wt.% of Ti as shown in Fig. 4. Presence of carbon and Iron in larger quantity makes the red mud more feasible to be used as filler material for enhancing the wear resistance of the polymer composites.

2.2 Fabrication of the Composite Specimen

The composites were prepared by resin transfer molding method. The mold cavity was made by 5 mm acrylic sheets with a size of 300 × 125 × 3 mm. The cavity surface was coated with mold releasing agent PVA, for easy removal of the composite. The calculated amount of 720 nm red mud was thoroughly mixed into a known measured quantity of resin and stirred well to get a homogeneous mixture. Cobalt naphthenate 0.5 wt.% and MEKP 2 wt.% was added to the mixture [1]. Then, it was mixed in a hand mixer and extreme care was taken to reduce air bubble generation. The mixture was kept in vacuum desiccators to confiscate the air entrapped in the mixer.

This resin red mud mixture was then gently poured into the mold through the left or right end. The mold was held in an inclined position while pouring the resin mixture in order to avoid the air bubble formation until the cavity was completely filled. Then, it was allowed to cure for about 24–26 h at ambient temperature and after that, the hardened composite sample was removed from the mold cavity. A similar procedure was adopted to prepare samples by adding the red mud particulates of size 612 nm, 475 nm, 263 nm, and 110 nm and also by varying the red mud content with 0.5, 1, 1.5, 2 and 2.5 wt.% for each case. A pure resin plate with no red mud particulate reinforcement was also prepared for comparison purpose. All the 26 composites samples prepared are designated in Table 1.

2.3 Mechanical Characterization

Density and void fraction, wear testing, scanning electron microscopy (SEM), X-ray diffraction (XRD) analysis, and Fourier transform infrared (FTIR) studies were carried out to explore the impact of the particle size and particle volume fraction on the tribological properties and they have been discussed here.

Fig. 1 Red mud ball milled for 18 h

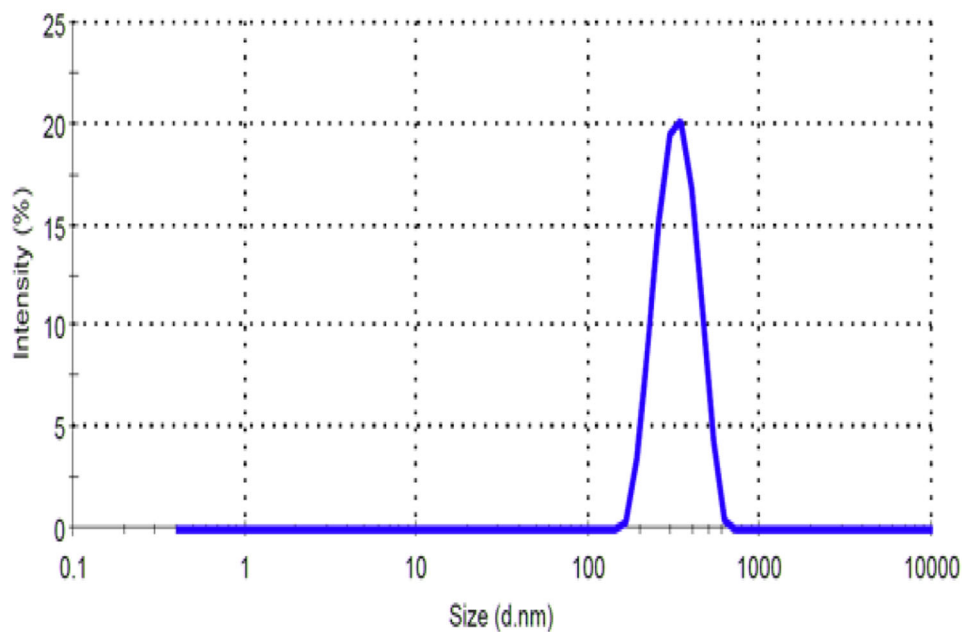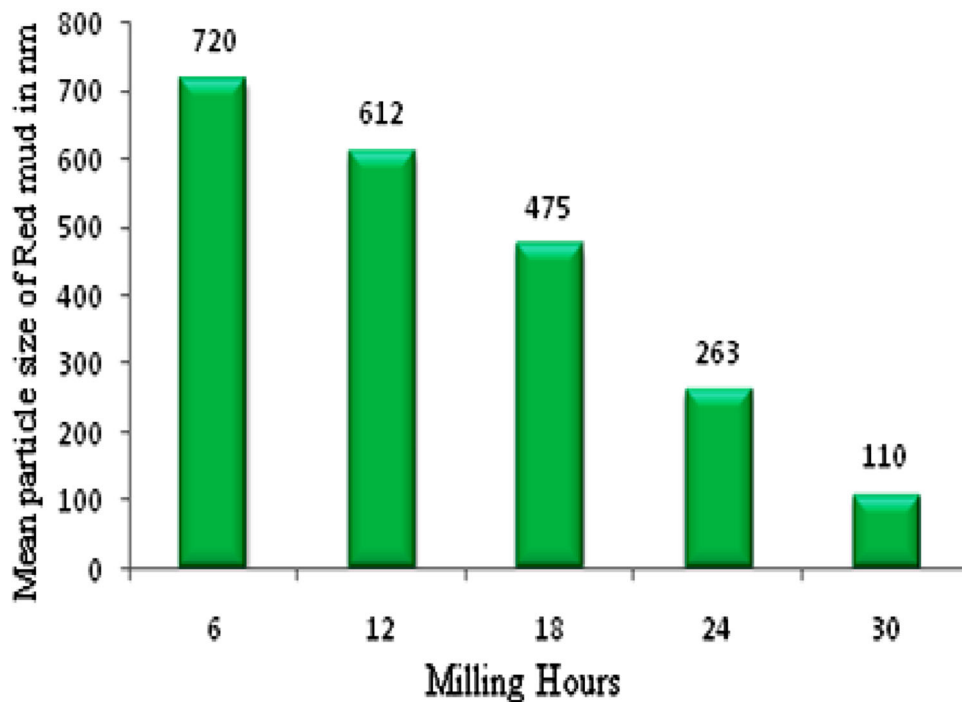**Fig. 2** Size distribution of particle for 18-h-milled red mud

Fig. 3 Mean particle size variation with milling hours variation

2.3.1 Density and Void Fraction

The experimental densities and theoretical densities are calculated based on the Archimedes principle and rule-of-mixture shown in Eq. 1. Both the densities of red mud filled polyester composites were compared by considering the respective volume fraction of voids.

$$\rho_t = \frac{1}{\left(\frac{W_m}{\rho_m}\right) + \left(\frac{W_p}{\rho_p}\right)} \qquad (1)$$

where W and ρ—weight fraction and density.

ρ_t—Theoretical density of the composite

The suffix p and m represent the particulate filler and the matrix, respectively. The density of the matrix (ρ_m) was found to be 1.22 g/cm^3 and that of the red mud particle was 2.53 g/cm^3 by measuring their mass and volume. The

Fig. 4 SEM–EDAX showing the chemical composition of the red mud particle

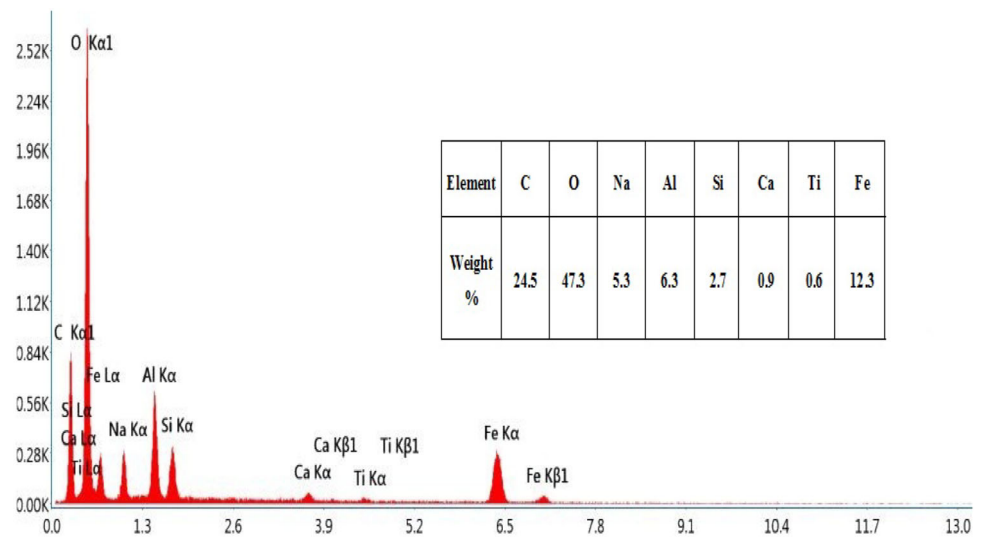| Element	C	O	Na	Al	Si	Ca	Ti	Fe
Weight %	24.5	47.3	5.3	6.3	2.7	0.9	0.6	12.3

Table 1 Nomenclature of the prepared composites sample (Red mud: RM)

Nomenclature of composite sample	Specific nomenclature of composite specimens	Average red mud particle size (nm)	Constituent of the composite
P	P	–	0% RM + Polyester
RA	RA1	720	0.5% RM + Polyester
	RA2		1% RM + Polyester
	RA3		1.5% RM + Polyester
	RA4		2%RM + Polyester
	RA5		2.5% RM + Polyester
RB	RB1	612	0.5% RM + Polyester
	RB2		1% RM + Polyester
	RB3		1.5% RM + Polyester
	RB4		2% RM + Polyester
	RB5		2.5% RM + Polyester
RC	RC1	475	0.5% RM + Polyester
	RC2		1% RM + Polyester
	RC3		1.5% RM + Polyester
	RC4		2% RM + Polyester
	RC5		2.5% RM + Polyester
RD	RD1	263	0.5% RM + Polyester
	RD2		1% RM + Polyester
	RD3		1.5% RM + Polyester
	RD4		2% RM + Polyester
	RD5		2.5% RM + Polyester
RE	RE1	110	0.5% RM + Polyester
	RE2		1% RM + Polyester
	RE3		1.5% RM + Polyester
	RE4		2% RM + Polyester
	RE5		2.5% RM + Polyester

experimental density (ρ_e) of fabricated composite material was determined by Archimedes principle by immersing the composite sample in water of known density. Both the experimental and theoretical densities thus determined

were compared and the void fraction of the composites was found out. The composites' void volume fraction (V_v) is determined by the following equation (Eq. 2.)

$$V_v = \frac{t - e}{t} \tag{2}$$

2.4 Wear Testing

Wear is continuous deletion or deformation of material at solid surface. The pin-on-disk apparatus is generally used to study the dry sliding wear properties of the composites. Figure 5 shows the apparatus used in this study. The samples of 10 × 10 × 3 mm size were cut from the plate according to ASTM G99-95 standards. Proper contact with the counter surface was essential for the tribological studies, and the same was ensured by rubbing against Silicon Carbide paper of 600 grades. Acetone soaked soft paper was used to clean the disk surface which was made of EN 8 carbon steel and the samples.

The tests were carried out at the environmental condition of 27 °C and a relative humidity of 43%. The weighed composite sample was held stationary over the rotating disk at a sliding distance kept as 3000 m and tract diameter as 80 mm. 30 N of normal force was applied at a constant sliding velocity of 3 m/s. Specific wear rate was calculated by weight loss method.

The weights of the specimens were measured precisely before and after the tests. The following expression has been used to find out the specific wear rate on the basis of volume loss [22]:

$$K_S = \frac{\Delta M}{\rho L F_n} \left(\frac{mm^3}{Nm}\right) \tag{3}$$

Where, ΔM—Mass loss (g),
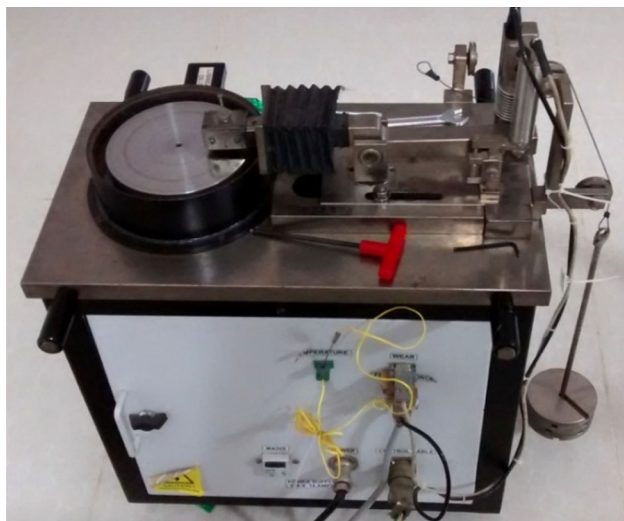ρ—Density (g/cm^3),

Fig. 5 Pin-on-disk setup

L—Sliding distance (m),
F_n—Applied normal load (N).

By taking the repeatability into account and for better accuracy, the results for wear tests have been acquired on six samples for each weight fraction and the mean values have been represented graphically.

2.5 Atomic Force Microscopy

Topography is a three-dimensional arrangement of physical attributes such as shape, height and depth of a surface in a region. The three-dimensional topography of red mud particle was analyzed by XE 70, Park Systems, a Korean-make Atomic Force Microscope.

2.6 Scanning Electron Microscopy (SEM)

The surfaces of the wear tested samples were gold sputtered, so as to convert it into a conducting material and then examined by scanning electron microscopes, i.e., Carl Zeiss EVO 18 and TESCAN VEGA3 SBU. The SEM micrographs of the worn-out tested samples were examined at suitable magnifications by subjecting them to a high voltage ranging from 10 to 15 kV.

2.7 X-Ray Diffraction (XRD) Analysis and Fourier transform Infrared (FTIR)

X'Pert PRO (PANalytical) X-ray diffractometer with Cu Kα radiation at the voltage of 40 kV was used for carrying out XRD analysis with the current like 30 mA. 2θ data from 10° to 80° was collected by following continuous scan mode. NICOLET IS10 spectrometer was used for Fourier transform infrared Spectrometry analysis by subjecting red mud powder sample to infrared light radiation at room temperature. The absorption took place when the vibrational frequency of the bond was equal to the infrared frequency. It recorded the interferogram and performed Fourier transform on the interferogram and the spectrum thus obtained. The functional compounds of the red mud were allocated, based on the analysis of the obtained absorption spectrum.

3 Results and Discussion

3.1 Characterization of Red Mud Particles

Red mud particles produced by the process of ball milling is characterized by the following methods to understand the shape, size, crystal structure, distribution, and its content.

3.1.1 Morphological Studies on Red Mud Particle

Scanning electron microscopic images have been used to study the morphology of red mud particle. Figure 6 shows the image of red mud particles milled for a duration of thirty hours in which it is observed that the size of the red mud particles is in the scale of a nanometer. It also validates the study carried out using particle analyzer. Also, it is found that the red mud particles are almost spherically shaped after ball milling. Yet, few agglomerations are also observed because of the fineness of the red mud particles.

As the size of the red mud particle decreases to nanoscale, the chances of it to get agglomerate increase. Agglomeration causes high concentration of resin red mud mixture during composite fabrication which makes the fabrication process more tedious. Figure 6 shows the micrograph of red mud particle with only little agglomeration which limits ball mill duration to 30 h. Fineness and possibility of agglomeration of the red mud particle need to be kept optimized to get desired polymer composite properties. Also Fig. 7 shows the difference between the red mud particle before ball mill and red mud particle after 6 h of ball milling process.

3.1.2 Atomic Force Microscopy

The atomic force microscopy (AFM) is used to analyze the 3D topography of the powdered red mud particles, and the result is shown in Fig. 8. Parameters such as volume, height, size, shape, aspect ratio and particle, three-dimensional topography information on surface morphology in angstrom scale to micron scale are measured from AFM. From Fig. 8, it is very clear that the red mud particles are in nanometer size and which is also similar to earlier observation carried by the particle analyzer shown in Fig. 2.
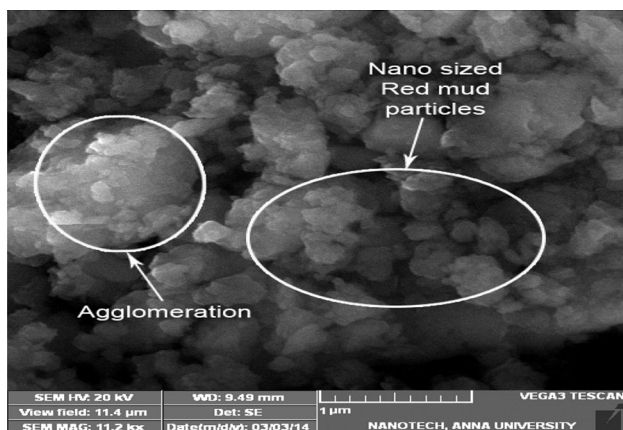

Fig. 6 SEM image of red mud particles milled for 30 h

3.1.3 Fourier Transform Infrared (FTIR) Spectroscopy

Figure 9 shows the Fourier transform infrared (FTIR) analysis of the absorption spectrum which analyzes the organic and inorganic components. The broadband occurs at around 953.59 cm^{-1}. This may be due to stretching vibrations of Si–O and O–Si–O. The absorption band around 1448.85 cm^{-1} may have occurred due to the presence of stretching vibrations of C=O [34], and the absorption band around 652.98 cm^{-1} confirms the presence of silicate groups which affect the tribological properties of the composites [35, 36]. The peaks at 3885.01 cm^{-1} and 1657.63 cm^{-1} represent the presences of O–H hydroxyl group with stretching and bending vibration modes. These peaks may have formed due to the water (H_2O) content in the raw material. The spectrum band formed at 3546.40 cm^{-1} represents the surface hydroxyl groups of Gibbsite (Al (OH)$_3$) which is also confirmed by the XRD analysis. Peaks at 2950.21 cm^{-1} and 1448.85 cm^{-1} represent the presence of Calcite (CaCo$_3$). The presence of band in FTIR spectrum between 950 and 970 cm^{-1} confirms the presents of Quartz (SiO$_2$). These results are consistent with the XRD analysis of the red mud particle.

3.1.4 X-Ray Diffraction (XRD) Graph

The crystal structure of the red mud particles has been identified by carrying out X-ray diffraction analysis. The XRD pattern of the red mud particle is shown in Fig. 10. The powder X-ray diffraction technique has been used in identifying the crystalline phases of the samples using monochromatized Cu–Kα (λ = 1.5056 A^0) on X-ray diffractometer. The data collection has been performed in the 2θ range of 10°–80° in steps of 0.1°/sec. Figure 10 shows the X-ray diffraction pattern of red mud. It is evident that the mineralogical components like hydroxycancrinite (Na$_8$Al$_6$Si$_6$)$_{24}$(OH)$_2$, gibbsite (Al (OH)$_3$), dicalcium silicate (Ca$_2$SiO$_4$), sodium aluminum silicate (Na (AlSiO$_4$)), quartz (SiO$_2$), ferrous sulfide (FeS), hematite (Fe$_2$O$_3$), calcite (CaCO$_3$), rutile phase titania (TiO$_2$) of red mud are present in the XRD pattern. The XRD patterns of the elements are referred from the Joint Committee on Powder Diffraction Standards (JCPDS) file.

3.2 Density and Void Fraction

The difference between the experimental density and the theoretical density is generally a measure of pores and voids presented in the composites. The theoretical and experimental density of the composite samples is obtained. The difference between them is calculated as a void fraction and is represented graphically in Fig. 11. From
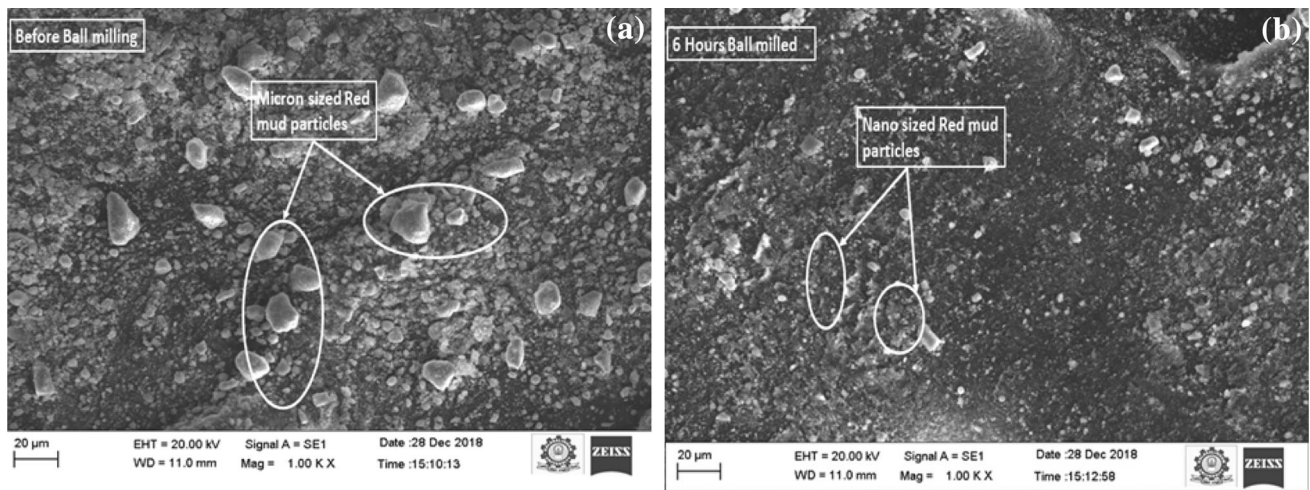
Fig. 7 SEM Image showing the red mud particle before (**a**) and after (**b**) ball milling process
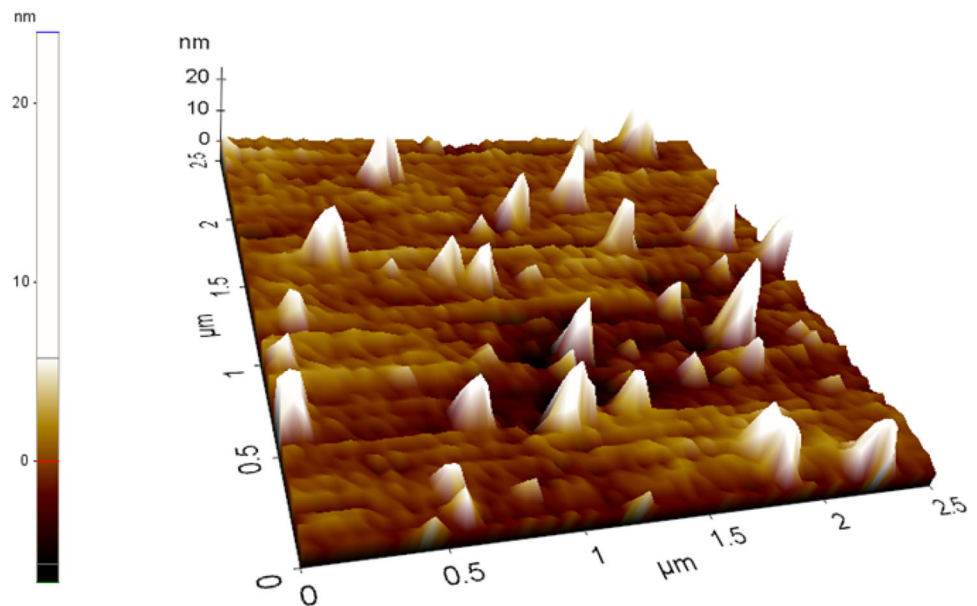

Fig. 8 Topography of the red mud particles

Fig. 11, it is observed that increase in weight fraction of red mud particle from 0.5 wt.% with an increment of 0.5 up to 2.5 wt.% in the composites has resulted in an increase in void fraction. The lowest void fraction is for 110 nm, and its value is found to be increasing with the increase in the size of the particle. The void fraction for 720 nm red mud particle polyester composite is greater than that of 110 nm red mud particle composites for all weight fractions. This may be due to entrapped air at the time of the composite preparation by resin transfer molding for sample designated as RE of particle size 110 nm.

The pure resin specimen also has void fraction due to the entrapped tiny air bubbles which may have been generated in the polyester resin during mixing. It is observed that the void fraction gradually increases when the wt.% of

the red mud particle rises to 2.5 wt.%. Again, if it increases past 2.5 wt.%, it may further drastically increase the void fraction which will degrade the mechanical properties of the composite material. Keeping this in mind, the particle content has been restricted within 2.5 wt.% for the present study.

3.3 Wear Test

3.3.1 Wear Rate and Coefficient of Friction

The influence of particle size and the particle loading on the specific wear rate and coefficient of friction of red-mud-based polymer composites at various wt.% of red mud have been studied, and the results are presented in Figs. 12
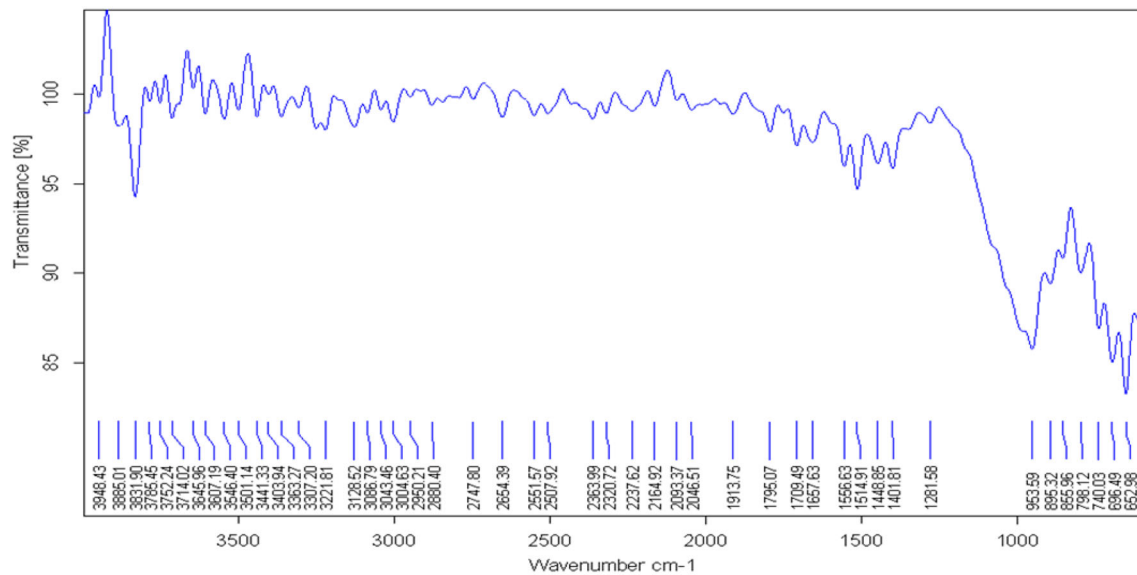
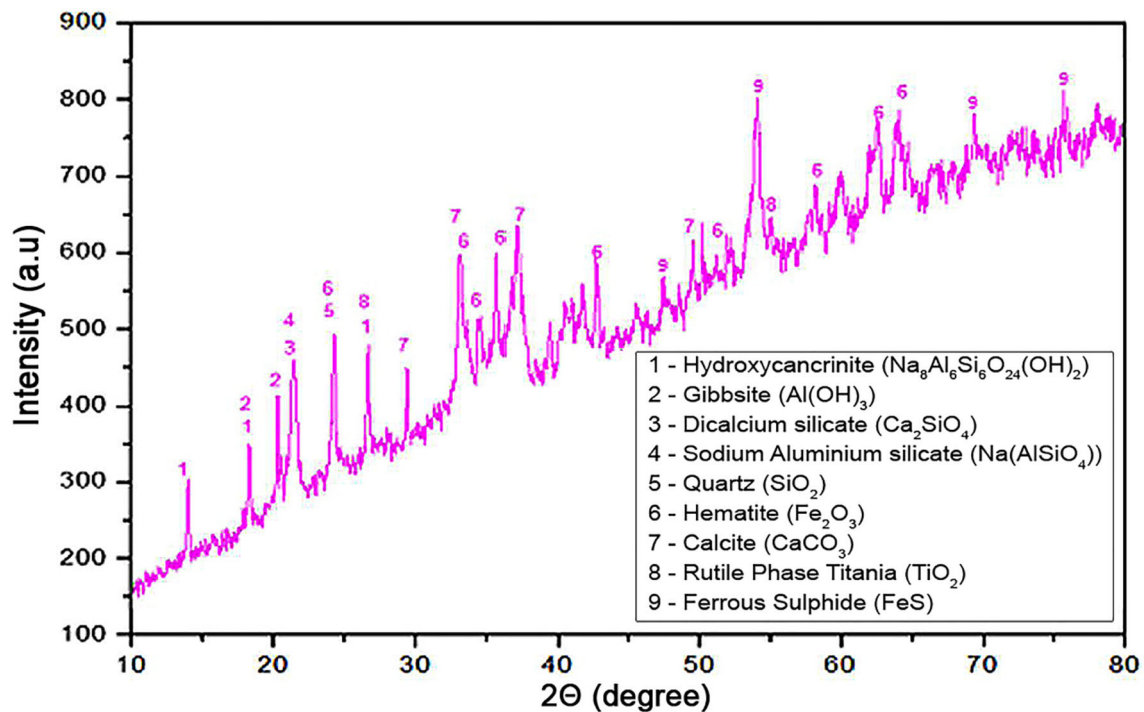**Fig. 9** FTIR Spectroscopy of red mud particles

Fig. 10 XRD of red mud particles

and 13. The experiment has been carried out by maintaining a sliding distance of 3000 m, with a normal load of 30 N at a velocity of 3 m/s. The specific wear rate of the cured virgin sample with no reinforcement has been reported to be 22.02×10^{-6} mm^3/Nm and the coefficient of friction as 0.559. The specific wear rate demonstrates a decreasing trend due to the introduction of nano-sized red mud particle as reinforcement in the polyester resin. A similar trend is also observed for the coefficient of friction.

The specific wear rate and the coefficient of friction are 21.8×10^{-6} mm^3/Nm and 0.55, respectively, for the sample with 720-nm-sized red mud powder with 0.5 wt.%. Both properties decrease as the particle content increases, and it reaches 14.9×10^{-6} mm^3/Nm and 0.46 when the particle content is at 2.5 wt.%. It amounts to 31.65% and 16.36% for specific wear rate and coefficient of friction, respectively. A similar trend is seen for the particle loading range of 0.5–2.5 wt.% due to the reinforcement of the resin
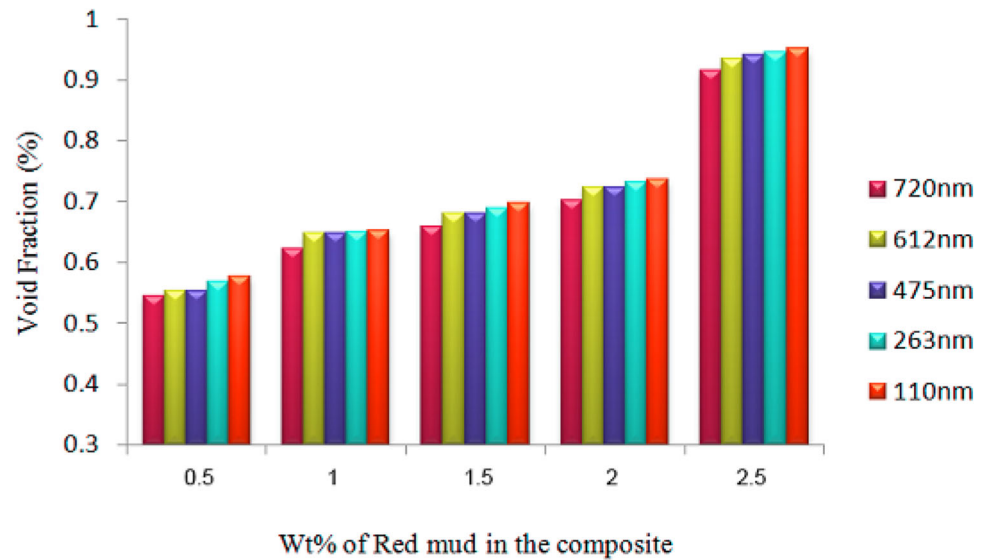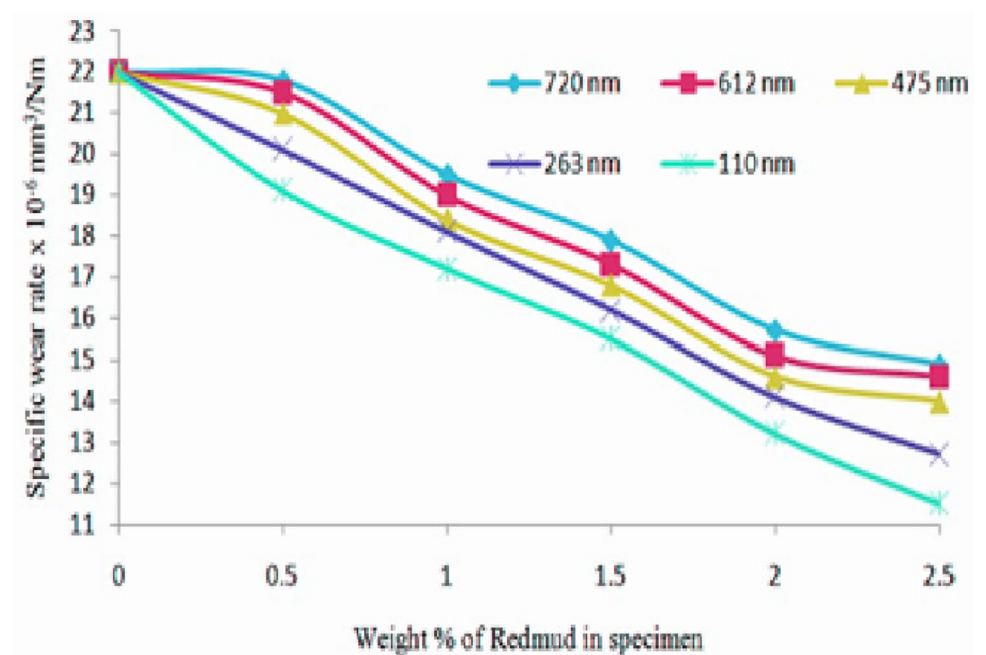
Fig. 11 Void fraction of composite specimen

Fig. 12 Specific wear rate variation for various red mud Wt.%


matrix by red mud particle whose size varies from 612 to 110 nm. The specific wear rate of 110 nm sized particle samples with a loading of 2.5 wt.% exhibits 47.72% reduction when compared to that of the cured virgin sample without any reinforcement.

It is seen that the specific wear rate of 0.5 wt.% particle loaded composite is found to decrease by 12.38% from 21.8×10^{-6} mm^3/Nm to 19.1×10^{-6} mm^3/Nm on reducing the particle size from 720 nm to 110 nm. Similarly, there is 16.36% reduction in the coefficient of friction and its value decreases from 0.55 to 0.46 when the particle size varies from 720 nm to 110 nm. In red mud particulate

loading of 2.5 wt.%, a 22.81%, reduction in specific wear rate is observed and its value decreases from 14.9×10^{-6} mm^3/Nm to 11.5×10^{-6} mm^3/Nm and the coefficient of friction reduces by 32.6% and its value decreases to 0.31 from 0.46 when the size of the particle decreases to 110 nm from 720 nm. The frictional coefficient of 110 nm size particle sample loaded with 2.5 wt.% RM particles exhibits 39.28% decrease upon comparing with cured pure resin samples. From these experimental results as observed from Figs. 12 and 13, it is understood that with a reduction in red mud particle size and along with an increase in particle loading, the specific wear rate

Fig. 13 Coefficient of Friction Variation for various red mud Wt.%
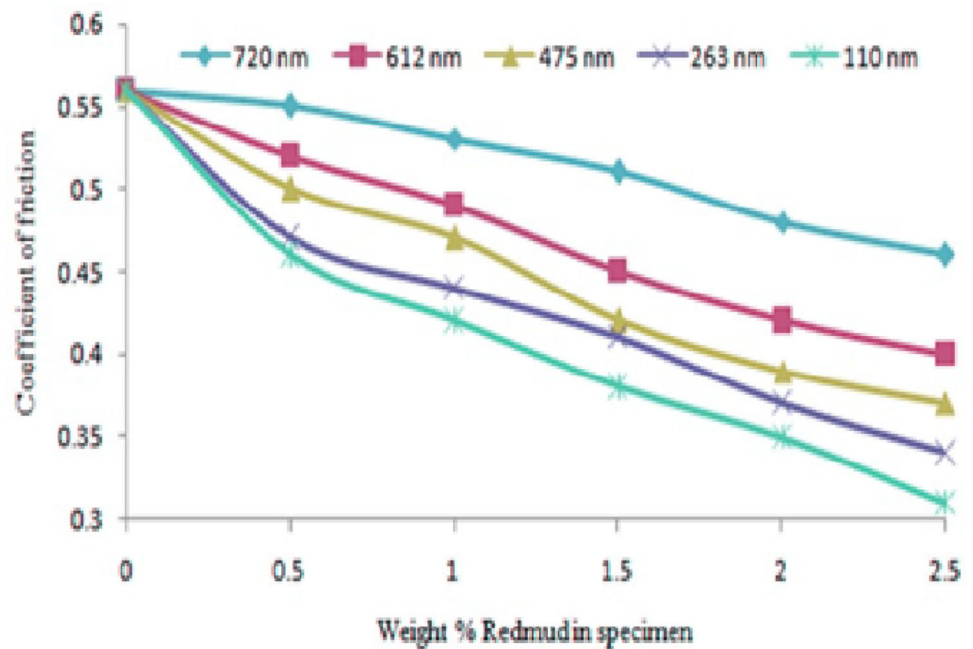
and coefficient of friction are found to be decreasing gradually. The presence of ferrous sulfide is confirmed in Sect. 3.1.4 XRD studies have a superior dry lubricating property which may be the reason for this decrease in coefficient of friction.

3.3.2 SEM Morphology of the Wear Surface

Scanning electron microscope image of the wear tested surfaces of pure polyester resin and red mud polyester composites are shown in Figs. 14, 15, 16, 17, 18 and 19. Figure 14 shows the image of wear tested neat polyester resin sample and the wear mechanism can be observed from it.
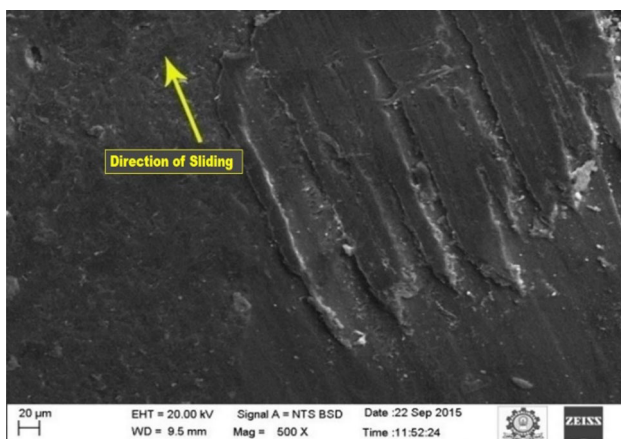

Fig. 14 SEM image of wear tested neat polyester resin sample

Severe wear and plastic deformation and deep grooves are observed on the surface of the tested sample because of the absence of reinforcement with RM particles. Adhesion, abrasion, fatigue, impact, electrical and chemical wear are the different types of wear mechanism that takes place in polymer. In this case, adhesion and abrasion are prominent. It is clear that severe plastic deformation and deep wear track, deep groove parallel to sliding direction are predominant in the wear direction as seen in the wear tested cured virgin polyester resin sample surface [37–39]. The virgin polyester resin sample has a coefficient of friction for (0.56) since it offers high resistance to the sliding motion which subsequently results in the rising of temperature of the worn-out surface. Due to this generation of heat, plastic deformation is created along the surface.

Deformation, microcutting, and high wear rate with rough surface are characterized as severe wear [37]. But for 720 nm size, on comparing particle loaded sample with 2.5 wt.% from Fig. 15b to 2.5 wt.% from Fig. 17a, there is comparatively lesser plastic deformation and deep grooves, which may be due to the self-lubricating property of ferrous sulfide content in red mud particles. Incorporation of red mud particles which contains ferrous sulfide reduces the friction coefficient. This results in the reduction of sliding resistance which again results in lesser wears with lesser plastic deformation in the wear direction.

SEM picture of the wear tested surface of composite sample of 612 nm RM particle with particle content of 0.5 wt.% and 2.5 wt.% are shown in Fig. 16a, b. Since the particle size is smaller, there exists an increase in contact surface area of the particulate surface. Also, the presence of
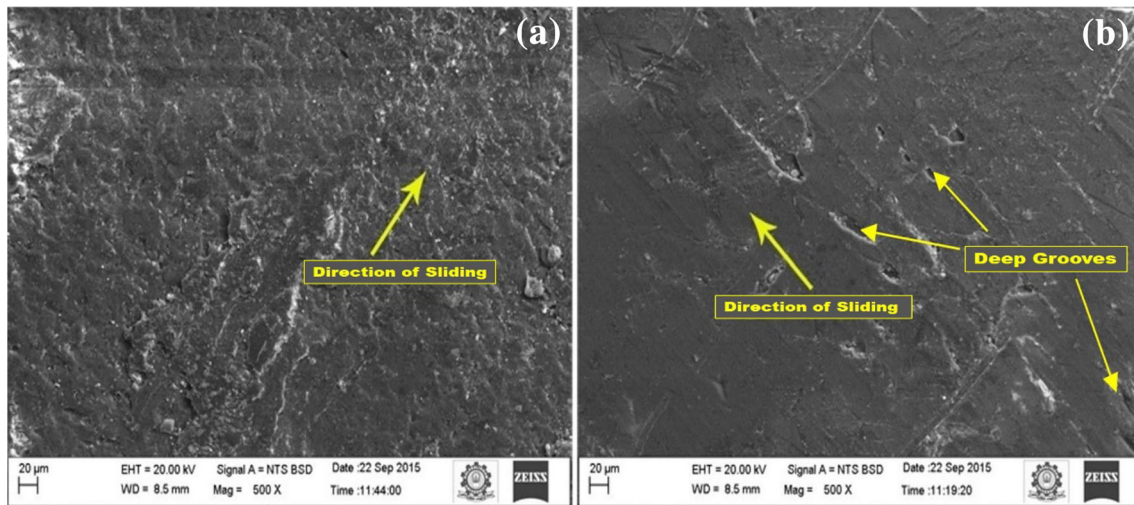
Fig. 15 SEM image of the tested composites reinforced with 720 nm red mud particulate with particle content of 0.5 wt.% (**a**) and 2.5 wt.% (**b**)
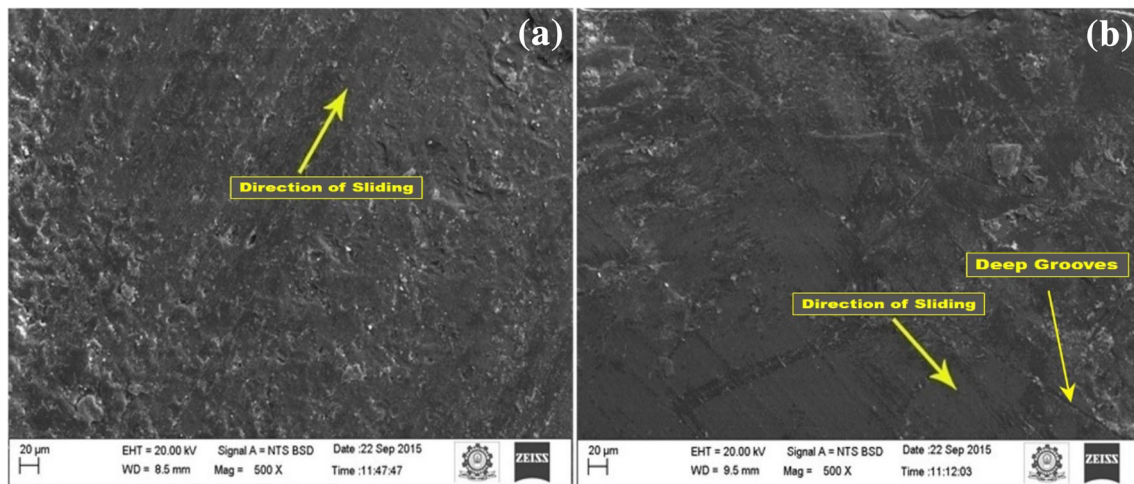

Fig. 16 SEM image of the tested composites reinforced with 612 nm red mud particulate with particle content of 0.5 wt.% (**a**) and 2.5 wt.% (**b**)
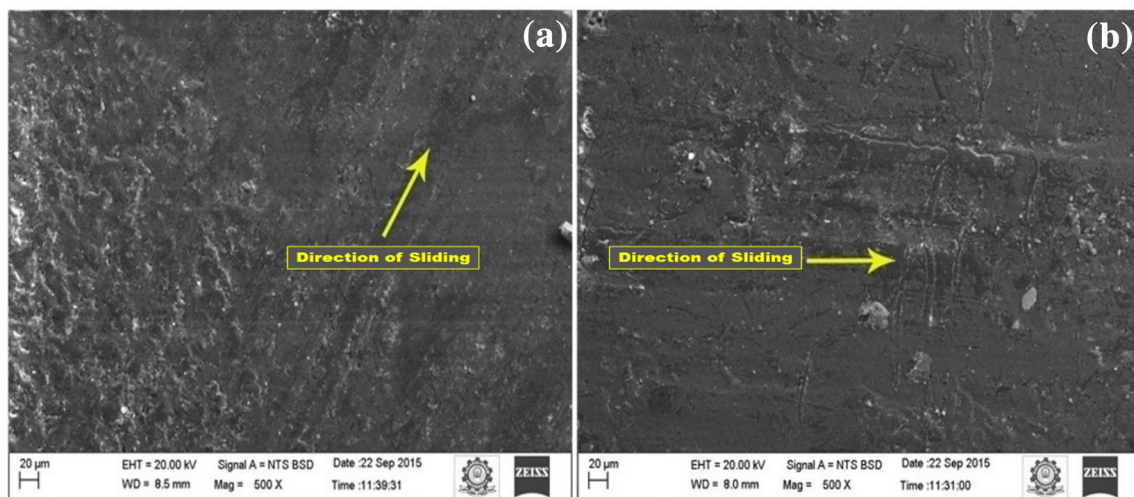

Fig. 17 SEM image of the tested composites reinforced with 475 nm red mud particulate having particle content of 0.5 wt.% (**a**) and 2.5 wt.% (**b**)
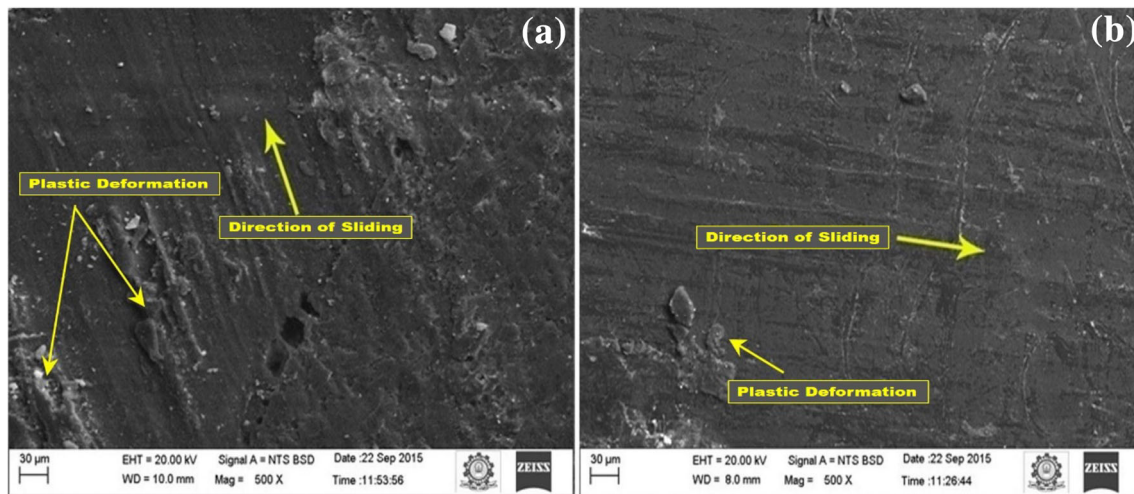
Fig. 18 SEM image of the tested composites reinforced with 263 nm red mud particulate having particle content of 0.5 wt.% (**a**) and 2.5 wt.% (**b**)
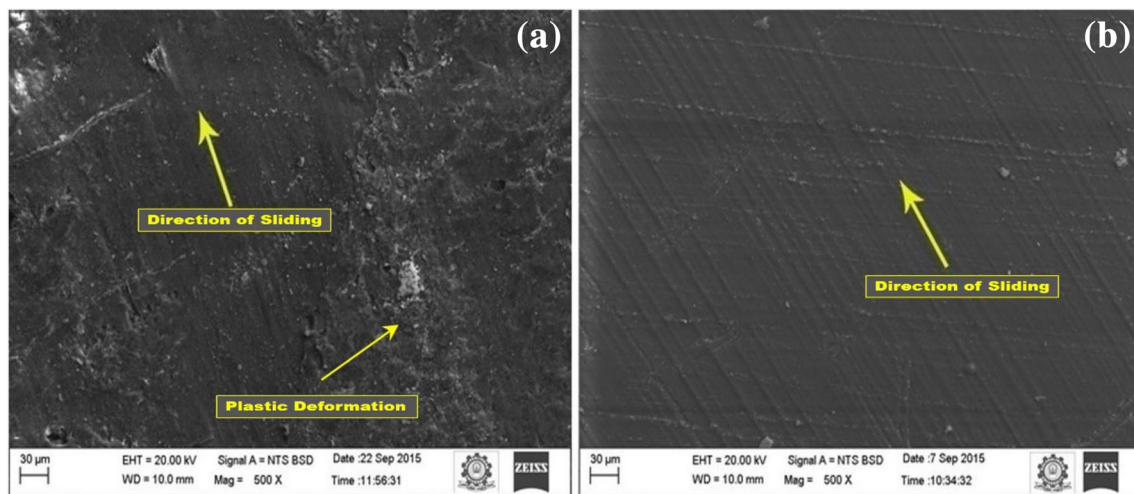

Fig. 19 SEM image of the wear tested composites reinforced with 110 nm red mud particulate of particle loading of 0.5 wt.% (**a**) and 2.5 wt.% (**b**)

ferrous sulfide in the red mud particle reduces the dry sliding friction. As the friction decreases, there exists a reduction in the surface temperature during wear. Because of this reduction in temperature which is generated due to sliding, there is the possibility of enhancement in bonding and reduction in plastic deformation. The effect of reduction in particle size and the resulting reduction in plastic deformation with a decrease in groove depth and detachment of RM particles from the matrix is noticed from Figs. 16, 17, 18 and 19. The void size and quantity of wear debris has been considerably reduced with the lowering of RM particle size. SEM images of worn-out surfaces of 2.5 wt.% loaded composites are shown from Figs. 15, 16, 17, 18 and 19b. From Figs. 15, 16, 17, 18 and 19a, lesser plastic deformation, smaller wear debris, shallow groves, and lesser voids are evident on comparing with the surfaces

of worn-out samples which is reinforced with lesser particle weight fraction (0.5 wt.%). Increasing the particle content leads to mild wear regime which is characterized by low wear rate with little damage and with low mass loss [37]. Smooth surface with shallow grooves, lesser plastic deformation, very few voids and very fine sized wear debris are visible in the tested sample with more particle loading and finer particle size as shown in Fig. 19b.

From Figs. 15b, 16, 17, 18 and 19b in which the RM particle content is kept as 2.5 wt.%, whereas the red mud particle size is varied from 720 to 110 nm, it is apparent that the decrease in particle size has played a major role in friction reduction and thereby reducing plastic deformation and wear. From this, it is concluded that the reinforcement of smaller sized particles with higher particle content into the polymer resin reduces the wear rate and gives birth to a

Fig. 20 SEM EDAX image of 110 nm size, 2.5 wt.% red mud particle tested sample
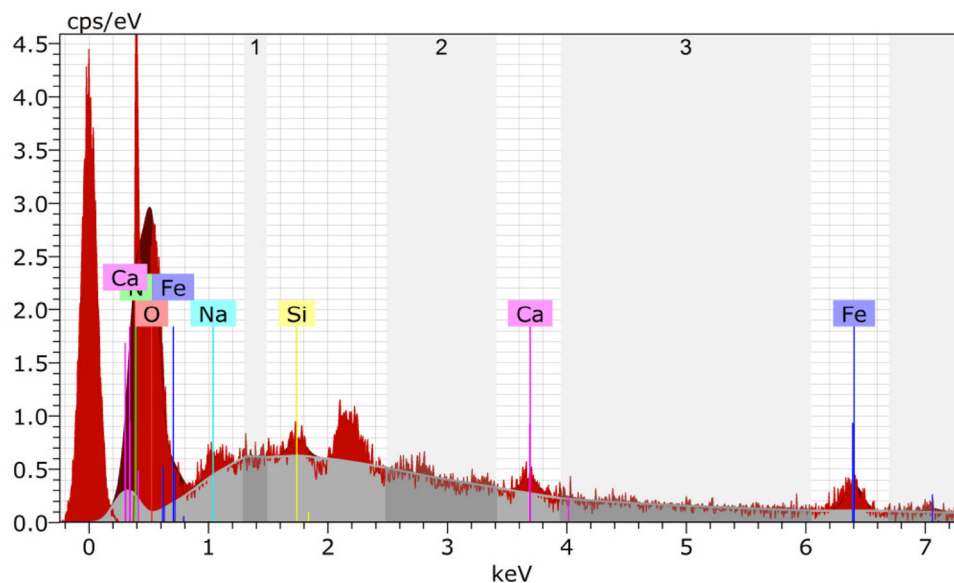
particulate composites material with enhanced tribological properties. The presence of ferrous sulfide content in the red mud is an added advantage since it has high melting point, low shear strength and provides the good hexagonal structure [40–42]. These properties of ferrous sulfide make it more compatible solid lubricant. Solid lubricant property of ferrous sulfide in red mud makes the composite wear resistant to certain extent, and hence, a reduction in wear is observed for increased red mud concentration. The wear rate also considerably reduces the particle size because of the presence of nano-sized red mud particles in the surface.

3.3.3 EDAX

From the SEM EDAX image of 110 nm size, 2.5 wt.% red mud particle composites tested as shown in Fig. 20, the presence of various compositions of red mud like Fe, Ca, Na, Si and O are clearly visible. The EDAX image confirms the presence of red mud in the fabricated composite sample. Generally, red mud contains the oxides of Fe, Si, Na, Ca, etc., in the form of Fe_2O_3, SiO_2, Na_2O, CaO, respectively. Hence, the dispersion of nano-sized red mud particles over the polyester matrix is justified.

4 Conclusion

In the present study, the ball mill was used to pulverize the red mud into nano-sized particles. Five different sizes were considered for experimentation. Characterization of Red mud particles was carried out by using Particle analyzer, XRD, FTIR, AFM, and SEM spectroscopy. Red mud

particles with five different Nano-sizes were used as reinforcement in a polymer matrix at five weight percent which resulted in 25 types of red mud particle-reinforced composites. The influences of the size of the particle and particle content on the tribological properties were studied. The surface morphology of the worn-out surface was analyzed using optical microscope and scanning electron microscope.

The research findings are summarized as follows:

- Specific wear rate of the red mud particulate composites decreased with increase in particle content as well as with a decrease in the size of the particle compared to the cured virgin polyester resin. 47.72% decrease in wear rate was observed for the composite with 2.5 wt.%, 110 nm sized red mud particle compared to cured pure resin.
- The frictional coefficient of red mud particulate-reinforced composite sample decreased when the particle content increased while decreasing the particle size on comparing with cured pure polyester resin. The coefficient of friction of the sample reinforced with 110 nm size and 2.5 wt.% red mud particle got decreased by 39.28% compared to that of cured pure polyester resin.
- This type of composite materials reinforced with smaller sized RM particle at higher particle content may be suitable for applications where good wear resistance is a vital one.

References

1. Richard S, SelwinRajadurai J and Manikandan V, *J. Tribol.* **139** (2016) 012202.
2. Arumugaprabu V, Uthayakumar M, Manikandan V, Rajini N and Jeyaraj P, *Mater. Des.* **64** (2014) 270.
3. Satheesh Raja R, Manisekar K and Manikandan V, *Mater. Des.* **55** (2014) 499.
4. Manikandan V, WinowlinJappes J, Suresh Kumar S and Amuthakkannan P, *Compos. Part B* **43** (2012) 812.
5. Ding M, Liu J, Liu B, Wang X, Li T and Cao D, in *Proceedings of SAE-China Congress 2015: Selected Papers* (2015) 297.
6. George P, Bhowmik S, Abraham M, Sriram P, Pitchan M, and Ajeesh G, *P. I. MECH. ENG. L J. MAT* (2016) https://doi.org/10.1177/1464420716660874.
7. Chauhan S and Thakur S, *Mater. Des.* **51** (2013) 398.
8. Arumugaprabu V, Manikandan V and Uthayakumar M, *IJE TRANSACTIONS B Appl.* **27** (2014) 1741.
9. Prabu, V.A, Manikandan V and Uthayakumar M, *P. I. Mech. Eng. L J. Mat* **227** (2013) 143.
10. Akinci A, Akbulut H and Yilmaz F, *Polym. Plast. Technol. Eng.* **46** (2007) 31.
11. Ahmed K, *J. Adv. Res.* **6** (2015) 225.
12. Rout A and Ray S, *Compos. Mech. Comput. Appl. Int. J.* **5** (2014) 259.
13. Mallakpour S and Khadem E, *Prog. Polym. Sci.* **51** (2015) 74.
14. Mittal G, Dhand V, Rhee K, Park S and Lee W, *J. Ind. Eng. Chem.* **21** (2015) 11.
15. Gao Z and Zhao L, *Mater. Des.* **66** (2015) 176.
16. Sharma S, Bijwe J, Panier S and Sharma M, *Wear* **332** (2015) 863.
17. Vaisakh S, Peer Mohammed A, Hassanzadeh M, Tortorici J, Metz R and Ananthakumar S, *Polym. Adv. Technol.* **27** (2016) 905.
18. Jia Z, Hao C, Yan Y and Yang Y, *Wear* **338** (2015) 282.
19. Wang W and Liu T, *J. Appl. Polym. Sci.* **109** (2008) 1654.
20. Tjong S C and Bao S, *e-Polymers* **7** (2007) 1618.
21. Liu Y and Kontopoulou M, *Polymer* **47** (2006) 7731.
22. Suresha B, Ravi Kumar B, Venkataramareddy M and Jayaraju T, *Mater. Des.* **31** (2010) 1993.
23. Richard S, Rajadurai J S and Manikandan V, *Int. J. Polym. Anal. Charact.* **21** (2016) 462.
24. Lin J, *Composites Part B* **38** (2007) 79.
25. Sun T, Fan H, Wang Z, Liu X and Wu Z, *Mater. Des.* **87** (2015) 10.
26. Bahadur S and Sunkara C, *Wear* **258** (2005) 1411.
27. Chang L, Zhang Z, Ye L and Friedrich K, *Tribol. Int.* **40** (2007) 1170.
28. Kurahatti R V, Surendranathan A O, Srivastava S, Singh N, Kumar A R and Suresha B, *Mater. Des.* **32** (2011) 2644.
29. Samal S, Ray A K and Bandopadhyay A, *Int. J. Miner. Process.* **118** (2013) 43.
30. Kumar A and Kumar S, *Constr. Build. Mater.* **38** (2013) 865.
31. Pontikes Y, Vangelatos I, Boufounos D, Fafoutis D and Angelopoulus G N, *Adv. Sci. Technol.* **45** (2006) 2176.
32. Liu Y, Lin C and Wu Y, *J. Hazard. Mater.* **146** (2007) 255.
33. Pinnock W R, Gordon J N, *J. Mater. Sci.* **27** (1992) 692.
34. Nath H, Sahoo A, *Int. J. Appl. Bioeng.* **8** (2014) 1.
35. Nan F, Xu Y, Xu B, Gao F, Wu Y and Li Z, *Tribol. Int.* **81** (2015) 199.
36. Singh D, Thakre G D, Sivakumar Konathala L N and Prasad V V D N, *Adv. Tribol.* **2016** (2016) 1901493.
37. Sun W, Xuan X, Li L and An J, *Material*s **11** (2018) 505.
38. Bermudez M-D, Carrion-Vilches F J and Martinez-Nicolas C, *J. Appl. Polym. Sci.* **831** (1999) 74.
39. M-D Bermudez, Carrion-Vilches FJ and Martinez-Mateo I, *J. Appl. Polym. Sci.* **81** (2001) 2426.
40. Fu S Y, Feng X Q, Lauke B and Mai Y W, *Compos. Part B* **39** (2008) 933.
41. Skarvelis P and Papadimitriou G D, *Surf. Coat. Technol.* **203** (2009) 1384.
42. Zhang G, Yin Y and Li J, *J. Mater. Res.* **32** (2017) 354.